Short communication

A novel nano-sulfur/polypyrrole/graphene nanocomposite cathode with a dual-layered structure for lithium rechargeable batteries

CrossMark

Yongguang Zhang, Yan Zhao, Aishuak Konarov, Denise Gosselink, Hayden Greentree Soboleski, P. Chen*

Department of Chemical Engineering, University of Waterloo, 200 University Avenue West, Waterloo, Ontario N2L3G1, Canada

HIGHLIGHTS

- A nano-sulfur/polypyrrole/graphene nanosheet composite was synthesized.
- Nano-S/PPy/GNS shows improved cycling and rate performance as sulfur cathode.
- Nano-S/PPy/GNS delivers 1415.7 mAh g^{-1} initial specific capacity at 0.1 C rate.

ARTICLE INFO

ABSTRACT

A method for synthesizing nano-sulfur/polypyrrole/graphene nanosheet (nano-S/PPy/GNS) ternary composite with a dual-layered structure is described. By taking advantage of both capillary force driven self-assembly of polypyrrole on graphene nanosheets and adhesion ability of polypyrrole to sulfur, we develop a stable and ordered nano-S/PPy/GNS composite cathode for lithium/sulfur (Li/S) batteries. The high dispersion of nanoscopic sulfur on the surface of PPy/GNS composite and good electrical conductivity of GNS seems to benefit the sulfur utilization and the reactivity of the composite. Furthermore, PPy plays an important role in retarding diffusion of polysulfides out of the electrode. The resulting nano-S/PPy/GNS composite cathode delivers a high initial capacity of 1415.7 mAh g^{-1}, remaining a reversible capacity of 641.5 mAh g^{-1} after 40 cycles at 0.1 C rate.

© 2013 Elsevier B.V. All rights reserved.

1. Introduction

In recent years, great efforts have been devoted to develop electric vehicles (EVs) in an attempt to reduce dependence on the limited fossil fuel resources and to decrease greenhouse gas emissions. The development of rechargeable lithium batteries with high-energy, high-power density and adequate safety is crucial for the introduction of such power storage devices into the new EV market [1–3]. Sulfur is a very attractive candidate as a cathode material due to its high theoretical specific capacity of 1672 mAh g^{-1}, based on the complete reaction of sulfur with lithium metal to form Li_2S [4–6]. In addition, sulfur has the advantages of abundant resources, low cost, and environmental friendliness [7]. However, the insulating character of sulfur and the solubility of intermediate polysulfides in organic liquid electrolytes, which causes rapid capacity loss upon repeated cycling, restrict the practical application of Li/S batteries [8,9]. Various carbonaceous [4–16] and conductive polymer materials [7,17–21] have been used to composite S, in an attempt to improve electrical conductivity and reduce the dissolution of lithium polysulfides.

Conducting polymers, such as polypyrrole (PPy) [20,21], polyaniline [22] and polythiophene [23] have received great deal of attention because they can have different roles in improving the performance of the sulfur cathode, due to their morphology and good electrochemical stability [23]. Polypyrrole is a specially promising matrix due to its high absorption ability to sulfur and polysulfides [20,21]. However, PPy/S composites also exhibit poor conductivity and rate capability, limiting its wide application [21].

Since the discovery of graphene in 2004, much attention has been drawn to its large surface area, superior electronic conductivity, and high mechanical flexibility [24–26]. Polypyrrole/graphene nanosheet (PPy/GNS) composites have been synthesized and used as electrochemical sensors and supercapacitors [27–34] and,

---

* Corresponding author. Tel.: +1 519 888 4567x35586; fax: +1 519 746 4979.
E-mail address: p4chen@uwaterloo.ca (P. Chen).

very recently, Wang and co-workers reported on a S-PPy/graphene multi-composite cathode for Li/S battery and obtained specific discharge capacities of 833 mAh g^{-1} at 0.1 C and 325 mAh g^{-1} at 1 C [35]. However, homogenous dispersion of large amounts of sulfur into this ternary composite was difficult and the resulting composites displayed non-uniform distribution of the sulfur particles, which limited the interface kinetic activity and rate capability [36,37].

Herein, we report on the preparation of a composite cathode material composed of nano-sulfur/polypyrrole/graphene (nano-S/PPy/GNS) which exhibit a well developed dual-layered sheet structure. We demonstrate that the homogeneous dispersion of sulfur on the surface of composite cathode give rise to high initial sulfur utilization and interfacial stabilization.

2. Experimental

2.1. Material synthesis

Polypyrrole was synthesized from pyrrole monomer (Aldrich, 98% purity) by the chemical oxidative procedure [38], using FeCl$_3$ (Sigma–Aldrich, 97%) as an oxidant. Polypyrrole-coated graphene (PPy/GNS) was synthesized by *in situ* polymerization of pyrrole in the presence of graphene [29–32].

0.1 g graphene nanosheet (US research nanomaterials Inc) was first dispersed in a 40 mL mixture of methanol and acetonitrile (1:1 vol) by sonication (Fisher Scientific, FB120) at room temperature for 2 h. After addition of 0.2 g of pyrrole this solution was stirred for 0.5 h. Afterward, 15 mL of 0.5 mol L^{-1} FeCl$_3$ aqueous solution was added dropwise to the above solution with constant sonication at ambient temperature. The mixture was sonicated again for 2 h. The final precipitate of PPy/GNS was separated via filtration, thoroughly washed with deionized water and methanol, and then vacuum dried overnight at 70 °C.

To make nano-S/PPy/GNS composite, as-prepared PPy/GNS was added into a 6 g nano-sulfur suspension (US research nanomaterials Inc, 10 wt %). The mixture was dispersed homogeneously for 0.5 h using an ultrasonic homogenizer, and then dried in a vacuum oven at 65 °C for 6 h to remove the solvents. Finally, the mixture was heated to 150 °C and kept for 3 h in Ar gas atmosphere to obtain the nano-S/PPy/GNS composite, in which the sulfur content, determined using chemical analysis (CHNS, Vario Micro Cube, Elementar), was 52%.

2.2. Material characterization

The surface morphology of PPy/GNS and nano-S/PPy/GNS composite were examined by emission scanning electron microscopy (SEM, Leo-1530, Zeiss). The interior structures of GNS, PPy/GNS and nano-S/PPy/GNS composite were observed using transmission electron microscopy (TEM, CM10, Philips) at 60 kV and high resolution transmission electron microscopy (HRTEM, FEI TITAN 80–300) equipped with Energy Dispersive Spectroscopy (EDS).

2.3. Electrochemical measurements

The electrochemical performance of nano-S/PPy/GNS composite sample was investigated using coin-type cells (CR2025). The cell was composed of lithium metal anode and nano-S/PPy/GNS cathode separated by a microporous polypropylene separator (Celgard®) soaked in 1 mol L^{-1} solution of lithium bistrifluoromethanesulfonamide (LiTFSI) (Aldrich, 96% purity) in tetraethylene glycol dimethyl ether (Aldrich, 99% purity) electrolyte. The composite cathode was prepared by mixing 80 wt% nano-S/PPy/GNS, 10 wt% polyvinylidene fluoride (PVDF) (Kynar, HSV900) as a binder and 10 wt% acetylene black (MTI, 99.5% purity) conducting agent in 1-methyl-2-pyrrolidinone (NMP, Sigma–Aldrich, ≥99.5% purity). The resultant slurry was coated onto Al foils and dried at 60 °C under vacuum overnight. The cathode material loading in each electrode was about 2 mg cm^{-2}. The coin cells were assembled in a MBraun glove box filled with high purity argon (99.9995% purity). The cells were tested galvanostatically on a multichannel battery tester (BT-2000, Arbin Instruments) between 1 and 3 V vs. Li$^+$/Li electrode at different current densities. Applied currents and specific capacities were calculated on the basis of S (theoretical specific capacity 1672 mAh g^{-1}) weight in the cathode. Cyclic voltammetry (CV) was performed with a potentiostat (VMP3, Biologic) between 1 and 3 V vs. Li$^+$/Li at a scanning rate of 0.5 mV s^{-1}. All electrochemical measurements were performed at room temperature.

3. Results and discussion

3.1. Properties of PPy/GNS and nano-S/PPy/GNS composite

The surface morphology of the PPy/GNS and nano-S/PPy/GNS composites is depicted in the SEM micrographs (Fig. 1a and b). PPy is formed and fixed to the surface of GNS after polymerization as shown in Fig. 1a. Pyrrole monomers are adsorbed onto the larger surface of GNS *via* π–π interactions, hydrogen bonds and Van der Waals interactions [28] serving as anchor points to the forming polymer. As for the nano-S/PPy/GNS composite (Fig. 1b), it forms irregular stacks of interlaced nanosheet-like structure, leading to a rough surface, densely covered with sulfur particles. This probably stems from the high absorption ability of PPy to sulfur [20,21]. The EDS mapping (Fig. 1c) shows the distribution of sulfur in the nano-S/PPy/GNS composite, confirming the highly homogeneous dispersion of nanoscopic sulfur on the surface of the parent PPy/GNS composite. Fig. 1(d–f) shows HRTEM images of as prepared PPy/GNS composite. At a high magnification (Fig. 1e), no obvious lattice fringes can be observed confirming the amorphous character of the PPy portion, in agreement with the literature data [39,40]. The EDS carbon and nitrogen mapping of PPy/GNS (Fig. 1f) show GNS homogeneously coated by PPy layer. Based on these observations, a possible mechanism for the composite formation is proposed as shown in Fig. 2. According to this mechanism, pyrrole is polymerized on the surface of the graphene nanosheets and the formed polypyrrole, which has a strong affinity toward sulfur, serves as an anchor point for the sulfur nanoparticles during the subsequent step. The resulting dual-layered composite has architecture hierarchical to the graphene nanosheet structure, quite different that obtained by Wang and co-workers [35].

3.2. Electrochemical properties of nano-S/PPy/GNS composite cathode material

Fig. 3 shows the two initial cycles cyclic voltammetry (CV) of a typical cell containing nano-S/PPy/GNS composite cathode. During the first cycle, three cathodic peaks and two anodic peaks are observed. The cathodic peak at 2.4 V can be assigned to the reduction of sulfur to polysulfides (Li$_2$S$_n$, $n \geq 4$) while the strong cathodic peak at 2.0 V is associated to the reduction of soluble polysulfides into Li$_2$S$_2$/Li$_2$S [41]. The appearance of a small peak at around 1.7 V is associated to the energy required to overcome the strong binding between the sulfur and the conductive matrix [42,43]. During the second cycle, the peak corresponding to the oxidation of polysulfides to S$_8$ becomes stronger and shifts to higher potential, indicating improvement of the reaction kinetics [44].
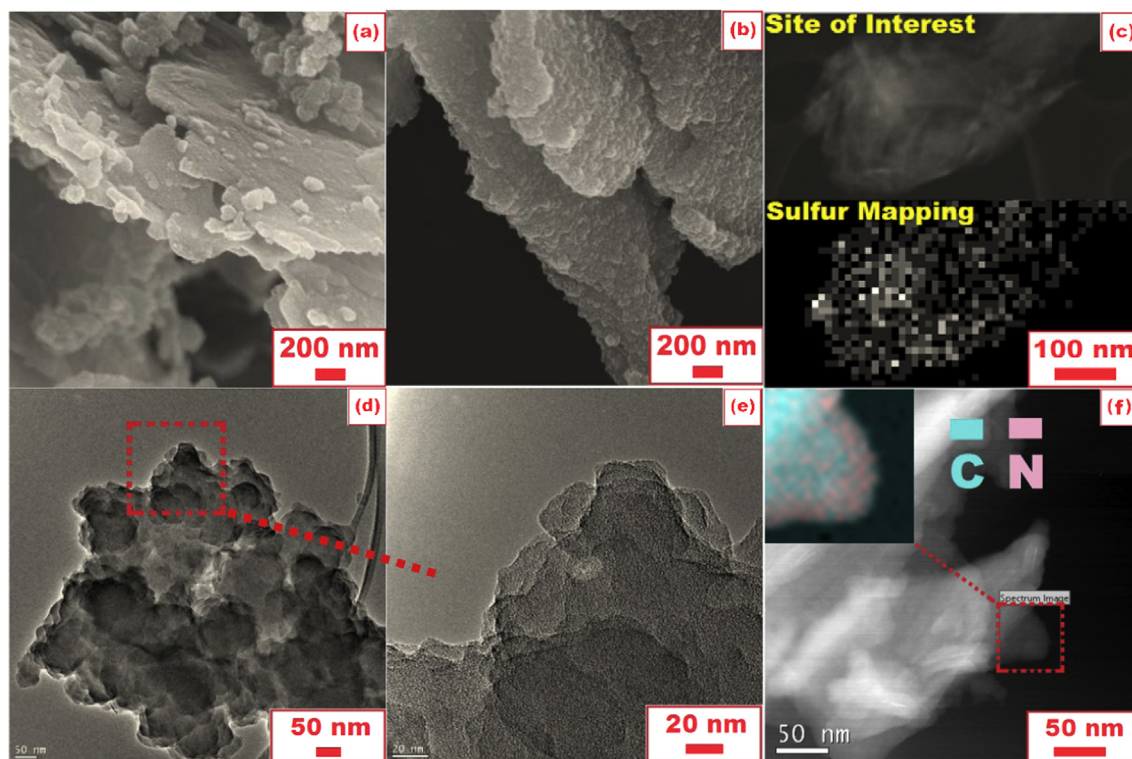
Fig. 1. (a and b) SEM image of PPy/GNS and nano-S/PPy/GNS composite samples; (c) EDS mapping showing distribution of sulfur (S) in composite of nano-S/PPy/GNS; (d, e and f) HRTEM images of PPy/GNS samples at different magnifications and EDS mapping showing distribution of carbon (C) and nitrogen (N).

The electrochemical performance of the nano-S/PPy/GNS composite as cathode materials in Li/S batteries was investigated by galvanostatic discharge/charge tests and the results are displayed in Fig. 4. The discharge curves show two plateaus that can be assigned to the two step reaction of sulfur with lithium, which is in good agreement with the CV data [16]. The first plateau at about 2.4 V is related to the formation of higher-order lithium polysulfides (Li_2S_n, $n \geq 4$), which are soluble in the liquid electrolyte. The following electrochemical transition of these polysulfides into lithium sulfide Li_2S_2/Li_2S is associated to a prolonged plateau around 2.0 V. The kinetics of this last reaction is slower than that of the polysulfide

formation, which is reflected by the length of the plateaus [45–48]. Fig. 5 presents the cycling performance of a Li/S cell containing nano-S/PPy/GNS composite cathode. The nanocomposite delivers a high initial discharge capacity of about 1415.7 mAh g^{-1} and maintains a reversible capacity of 641.5 mAh g^{-1} after 40 cycles at 0.1 C rate. This represents a better cycling performance than that observed for S/PPy composites without graphene, at a cycling rate twice as fast [20,21]. Furthermore, the coulombic efficiency higher or equal than 90% during the 40 cycles indicates that PPy in the composite plays the significant role of absorbing the polysulfides and suppressing the shuttle effect.
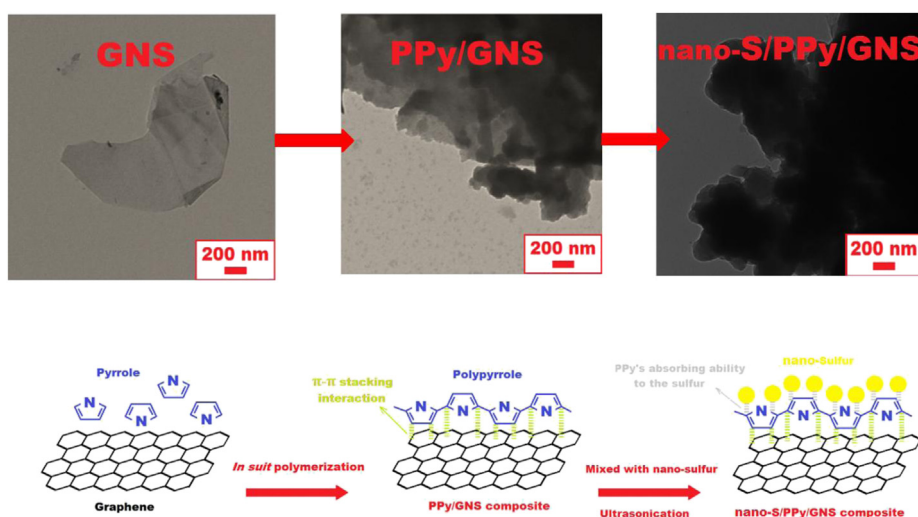

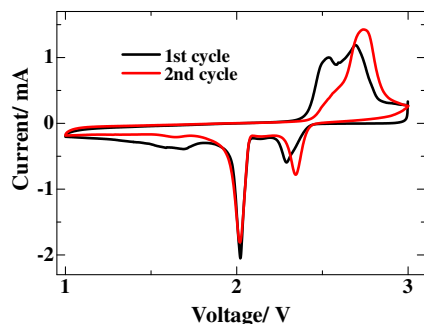**Fig. 2.** Schematic of the nano-S/PPy/GNS composite preparation.

Fig. 3. Initial CV profiles of nano-S/PPy/GNS composite, used as a cathode active material in the lithium half-cell. The measurement is conducted at a scan rate of 0.5 mV s^{-1} in the voltage range of 1.0–3.0 V vs. Li$^+$/Li.
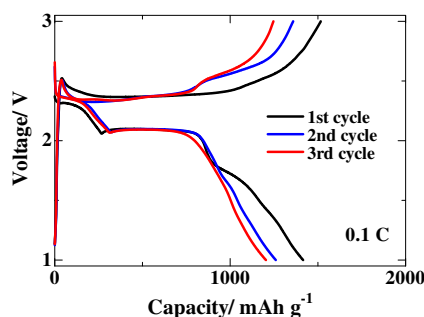

Fig. 4. Discharge/charge profiles of lithium cell with nano-S/PPy/GNS composite cathode at 0.1 C.
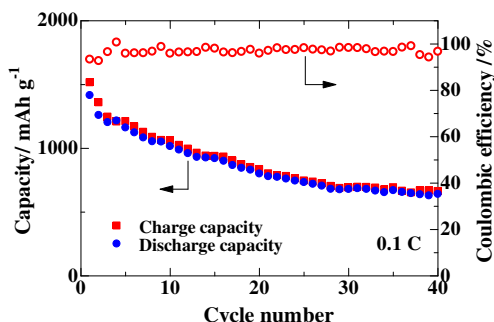

Fig. 5. Discharge/charge capacity and coulombic efficiency vs. cycle number for the nano-S/PPy/GNS lithium cell at 0.1 C.

To further investigate the electrochemical properties of the nano-S/PPy/GNS nanocomposite, a rate performance study was carried out as show in Fig. 6. Initial capacities of 988.7 mAh g^{-1} and 830.1 mAh g^{-1} were obtained at rates of 0.5 C and 1 C, respectively.
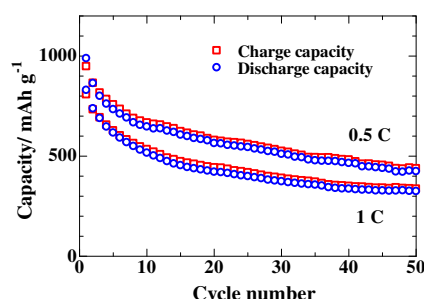

Fig. 6. Rate capability for the nano-S/PPy/GNS lithium cell.

After 50 cycles the capacity remained at 424.5 mAh g^{-1} and 324.7 mAh g^{-1}, showing the good rate capability of the nano-S/PPy/GNS composite cathode.

Based on our observations, we postulate that the combined effects of the individual components and dual-layered structure of the composite play a key role on its electrochemical performance. The high dispersion of nanoscopic sulfur layer on the surface of PPy/GNS composite contributes to the excellent high rate discharge capability of the sulfur cathode owing to the good electrical conductivity of GNS and good lithium ion transport path. Concomitantly, the PPy porous structure accommodates more volume changes during cycling and also plays an important role in retarding diffusion of polysulfides out of the electrode.

4. Conclusions

A method for fabricating a ternary nano-sulfur/polypyrrole/graphene nanosheet composite has been developed. The method, based on previous work to synthesize PPy/GNS composite by the *in situ* chemical polymerization of pyrrole on the graphene nanosheet, employs nanosized sulfur particle suspension to produce a novel cathode material with dual-layered structure. The electrochemical results show that graphene can provide an effective electron conduction path and the nano-S/PPy/GNS nanocomposite forms a stable dual-layered structure for the S electrode. PPy also has strong adhesion to the surface of graphene and absorb polysulfides into its porous structure. Consequently, the nano-S/PPy/GNS composite cathode exhibits improved cycling and rate performances for rechargeable lithium/sulfur batteries, with high initial sulfur utilization.

Acknowledgments

References

[1] M. Armand, J.M. Tarascon, Nature 451 (2008) 652–657.
[2] B. Kang, G. Ceder, Nature 458 (2009) 190–193.
[3] Y. Zhang, Y. Zhao, K.E.K. Sun, P. Chen, Open Mater. Sci. J. 5 (2011) 215–221.
[4] X. Ji, L.F. Nazar, J. Mater. Chem. 20 (2010) 9821–9826.
[5] P. Novak, K. Mueller, K.S.V. Santhanam, O. Haas, Chem. Rev. 97 (1997) 207–281.
[6] Y. Zhang, Z. Bakenov, Y. Zhao, A. Konarov, T.N.L. Doan, K.E.K. Sun, A. Yermukhambetova, P. Chen, Powder Technol. 235 (2013) 248–255.
[7] L. Yin, J. Wang, F. Lin, J. Yang, Y. Nuli, Energy Environ. Sci. 5 (2012) 6966–6972.
[8] J.A. Dean, Lange's Handbook of Chemistry, thirteenth ed., McGraw-Hill, New York, 1985.
[9] R.D. Rauh, F.S. Shuker, J.M. Marston, S.B. Brummer, J. Inorg. Nucl. Chem. 39 (1977) 1761–1766.
[10] J. Wang, S.Y. Chew, Z.W. Zhao, S. Ashraf, D. Wexler, J. Chen, S.H. Ng, S.L. Chou, H.K. Liu, Carbon 46 (2008) 229–235.
[11] Y. Zhao, Y. Zhang, Z. Bakenov, P. Chen, Solid State Ionics 234 (2013) 40–45.
[12] N.W. Li, M.B. Zheng, H.L. Lu, Z.B. Hu, C.F. Shen, X.F. Chang, G.B. Ji, J.M. Cao, Y. Shi, Chem. Commun. 48 (2012) 4106–4108.
[13] S. Dörfler, M. Hagen, H. Althues, J. Tübke, S. Kaskel, M.J. Hoffmann, Chem. Commun. 48 (2012) 4097–4099.
[14] S. Evers, L.F. Nazar, Chem. Commun. 48 (2012) 1233–1235.
[15] X.L. Li, Y.L. Cao, W. Qi, L.V. Saraf, J. Xiao, Z.M. Nie, J. Mietek, J.G. Zhang, B. Schwenzera, J. Liu, J. Mater. Chem. 21 (2011) 16603–16610.
[16] L.W. Ji, M.M. Rao, S. Aloni, L. Wang, E.J. Cairns, Y.G. Zhang, Energy Environ. Sci. 4 (2011) 5053–5059.

[17] J.L. Wang, J. Yang, C.R. Wan, K. Du, J.Y. Xie, N.X. Xu, Adv. Funct. Mater. 13 (2003) 487—492.
[18] J. Wang, J. Chen, K. Konstantinov, L. Zhao, S.H. Ng, G.X. Wang, Z.P. Guo, H.K. Liu, Electrochim. Acta 51 (2006) 4634—4638.
[19] Y. Zhang, Y. Zhao, A. Yermukhambetova, Z. Bakenov, P. Chen, J. Mater. Chem. A 1 (2013) 295—301.
[20] X. Liang, Y. Liu, Z.Y. Wen, L.Z. Huang, X.Y. Wang, H. Zhang, J. Power Sources 196 (2011) 6951—6955.
[21] Y. Zhang, Z. Bakenov, Y. Zhao, A. Konarov, T.N.L. Doan, M. Malik, T. Paron, P. Chen, J. Power Sources 208 (2012) 1—8.
[22] G.C. Li, G.R. Li, S.H. Ye, X.P. Gao, Adv. Energy Mater. 2 (2012) 1238—1245.
[23] F. Wu, S. Wu, R. Chen, J. Chen, S. Chen, Electrochem. Solid-State Lett. 13 (2010) A29—A31.
[24] Y. Jiang, Y. Xu, T. Yuan, M. Yan, Mater. Lett. 91 (2013) 16—19.
[25] K.S. Novoselov, A.K. Geim, S.V. Morozov, D. Jiang, Y. Zhang, S.V. Dubonos, I.V. Grigorieva, A.A. Firsov, Science 306 (2004) 666—669.
[26] F. Miao, S. Wijeratne, Y. Zhang, U.C. Coskun, W. Bao, C.N. Lau, Science 317 (2007) 1530—1533.
[27] S. Zhang, Y. Shao, J. Liu, I.A. Aksay, Y. Lin, Appl. Mater. Interfaces 3 (2011) 3633—3637.
[28] X.J. Lu, F. Zhang, H. Dou, C.Z. Yuan, S.D. Yang, L. Hao, L. Shen, L.J. Zhang, X.G. Zhang, Electrochim. Acta 69 (2012) 160—166.
[29] H.H. Chang, C.K. Chang, Y.C. Tsai, C.S. Liao, Carbon 50 (2012) 2331—2336.
[30] D. Zhang, X. Zhang, Y. Chen, P. Yu, C.H. Wang, Y. Ma, J. Power Sources 196 (2011) 5990—5996.
[31] C.H. Xu, J. Sun, L. Gao, J. Mater. Chem. 21 (2011) 11253—11258.
[32] S. Sahoo, G. Karthikeyan, G.C. Nayak, C.K. Das, Synth. Met. 161 (2011) 1713—1719.
[33] V. Chandra, K.S. Kim, Chem. Commun. 47 (2011) 3942—3944.
[34] S. Biswas, L.T. Drzal, Chem. Mater. 22 (2010) 5667—5671.
[35] W. Wang, G.C. Li, Q. Wang, G.R. Li, S.H. Ye, X.P. Gao, J. Electrochem. Soc. 160 (2013) A805—A810.
[36] J.J. Chen, Q. Zhang, Y.N. Shi, L.L. Qin, Y. Cao, M.S. Zheng, Q.F. Dong, Phys. Chem. Chem. Phys. 14 (2012) 5376—5382.
[37] Y. Zhang, Y. Zhao, T.N.L. Doan, A. Konarov, D. Gosselink, H.G. Soboleski, P. Chen, Solid State Ionics 238 (2013) 30—35.
[38] M.M. Chehimi, E. Abdeljalil, Synth. Met. 145 (2004) 15—22.
[39] J.T. Lei, W.B. Liang, C.R. Martin, Synth. Met. 48 (1992) 301—312.
[40] K. Cheah, M. Forsyth, V.T. Truong, Synth. Met. 94 (1998) 215—219.
[41] G. Zhou, D.W. Wang, F. Li, P.X. Hou, L. Yin, C. Liu, G.Q. Lu, I.R. Gentle, H.M. Cheng, Energy Environ. Sci. 5 (2012) 8901—8906.
[42] X. Liang, Z.Y. Wen, Y. Liu, H. Zhang, J. Jin, M. Wu, X.W. Wu, J. Power Sources 206 (2012) 409—413.
[43] B. Zhang, C. Lai, Z. Zhou, X.P. Gao, Electrochim. Acta 54 (2009) 3708—3713.
[44] B. Zhang, X. Qin, G.R. Li, X.P. Gao, Energy Environ. Sci. 3 (2010) 1531—1537.
[45] D. Marmorstein, T.H. Yu, K.A. Striebel, F.R. McLarnon, J. Hou, E.J. Cairns, J. Power Sources 89 (2000) 219—226.
[46] D.H. Han, B.S. Kim, S.J. Choi, Y. Jung, J. Kwak, S.M. Park, J. Electrochem. Soc. 151 (2004) E283—E290.
[47] H. Yamin, A. Gorenshtain, J. Penciner, Y. Sternberg, E. Peled, J. Electrochem. Soc. 135 (1988) 1045—1048.
[48] V.S. Kolosnitsyn, E.V. Karaseva, Russ. J. Electrochem 44 (2008) 506—509.